Polym. Bull. (2017) 74:5111–5128
DOI 10.1007/s00289-017-2010-6

ORIGINAL PAPER

The production and characterization of poly(lactic acid) fibers dyeable with anionic dyes using octaammonium polyhedral oligomeric silsesquioxane nanoparticle

Onur Baykus[1] · Asım Davulcu[1] · Mehmet Dogan[1]

Received: 20 October 2016 / Revised: 20 March 2017 / Accepted: 30 March 2017 /
Published online: 1 April 2017

Abstract In this study, acid dyeable poly(lactic acid) (PLA) fiber was produced with the addition of octaammonium polyhedral oligomeric silsesquioxane (OA-POSS) nanoparticle during the melt spinning. The tensile, thermal and morphological properties of the fiber samples were characterized by tensile testing, differential scanning calorimetry, scanning electron microscopy and transmission electron microscopy. Two different anionic dyes, a disulphonated 1:2 premetallised acid dye and monosulphonated non-metallised, were used. The effects of dyeing conditions including dyeing temperature and time, OA-POSS concentration, anionic dye types and concentrations were investigated on the dyeability properties of the PLA fiber samples. It was concluded that the percent crystallinity and the tensile strength of pure PLA fiber decreased as the added amount of OA-POSS increased. According to the dyeing results, the addition of OA-POSS greatly improved the dyeability of the PLA fiber with anionic dyes by introducing ion–ion interaction between the terminal ammonium groups of POSS nanoparticle and the sulphonyl groups of dye molecules.

Keywords Poly(lactic acid) fiber · Melt spinning · Dyeability · POSS nanoparticle · Anionic dye

Introduction

Poly(lactic acid) (PLA), a bio-based aliphatic polyester, is derived from agricultural sources like corn starch. It finds use in various textile applications such as household and industrial wipes, diapers, feminine hygiene products and disposable garments [1–3]. PLA fiber is commercially dyed with disperse dyes at low temperature in a

✉ Mehmet Dogan
mehmetd@erciyes.edu.tr

[1] Department of Textile Engineering, Erciyes University, 38039 Kayseri, Turkey

short time (typically 110 °C for 30 min) to prevent the loss of mechanical properties due to the low-melting point and the low hydrolytic stability. Thus, the dyeing yield of PLA fiber strongly depends on the disperse dye structure [2, 4–11]. For increasing the dye uptake of PLA fiber with disperse dyes, the synthesizing of the special dye molecules, the modification of the dyeing procedure and the modification of PLA fiber during the melt spinning are widely preferred methods in the literature [12–18].

In the literature, various modifiers were used during the melt spinning to improve the dye uptake of synthetic fibers to anionic and cationic dyes [19–27]. In these studies, amine based modifiers [21, 22, 26], polyamide [23, 24], organoclay [19, 20, 27], and silver nanoparticles [25] were used as functional filler for increasing the dyeability properties of synthetic fibers including polypropylene [19, 21–23, 26, 27], polyamide 6 [20], polyethylene terephthalate [25] and polytrimethylene terephthalate [24]. No study was found in the literature to improve the dyeability behavior of PLA fiber with anionic dyes during the melt spinning.

The aim of this study is to produce acid dyeable PLA fiber using octaammonium POSS (OA-POSS) nanoparticle. OA-POSS nanoparticle bears eight quaternary ammonium cations. The molecular structure of the OA-POSS nanoparticle is shown in Fig. 1. This modification relies on the introduction of the cationic group as dye receptor sites into PLA fiber structure during the melt spinning. The produced PLA fibers are characterized using tensile testing, differential scanning calorimeter (DSC). The state of the OA-POSS dispersion in PLA matrix is investigated via scanning electron microscopy (SEM) and transmission electron microscopy (TEM). The effect of the dyeing conditions including dyeing temperature and time, acid dye type and concentration, and OA-POSS concentration are investigated on the dyeability properties of PLA fiber samples. The wash and light fastness properties of the selected PLA fiber samples are also investigated.

Experimental

Materials

Fiber grade PLA with the trade name of 6202D was purchased from Cargill–Dow (Nebraska, USA). The density is 1.24 g/cm^3 (ASTM D792) and the melt flow index is 15–30 g/10 min (2.16 kg, 210 °C), as provided by the supplier. OA-POSS was purchased from Hybrid Plastics Inc. (Hattiesburg, USA). Two different acid dyes,

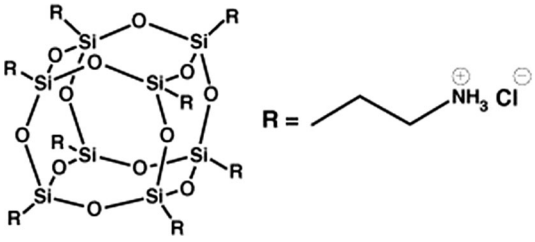

Fig. 1 The molecular structure of the OA-POSS nanoparticle

Acid Blue 193 and Acid Blue 62, were obtained from SETAS Colorcenter (Tekirdag, Turkey). Acid Blue 193 is a disulphonated 1:2 premetallised acid dye. Acid Blue 62 is a monosulphonated non-metallised acid dye. The chemical structures of acid dyes are shown in Fig. 2. Sandoclean PC, nonionic surfactant agent, was obtained from Clariant (Istanbul, Turkey). Analytical grade acetic acid was purchased from Sigma-Aldrich.

Production of nanocomposite fibers

The nanocomposite fibers were produced in a two-step extrusion process and a one-step hot drawing process. To prevent the degradation caused by humidity, PLA was dried at 80 °C for 8 h under vacuum before the extrusion process [28, 29]. A corotating twin screw extruder (*L*/*D*: 12) (Gulnar Makina, Istanbul, Turkey) coupled to a drawing unit was used during the fiber spinning process. The diameter of the die was 0.5 mm. The first step of the extrusion process was conducted for obtaining the nanocomposite structure. The mixing PLA with OA-POSS (0.5, 1 and 3 wt%) was conducted at 100 rpm with a temperature profile of 120–160–180–200–210–210 °C. In the second step, the pellets produced from the first extrusion process were fed into the same extruder and the extruder was brought to force-controlled mode to ensure a uniform

Fig. 2 The chemical structures of the acid dyes

Acid Blue 193

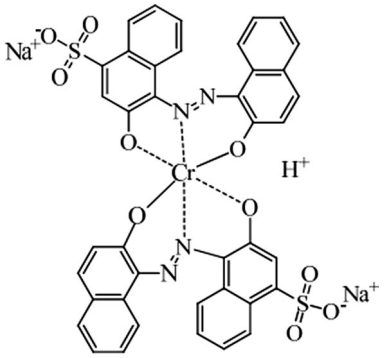

Acid Blue 62

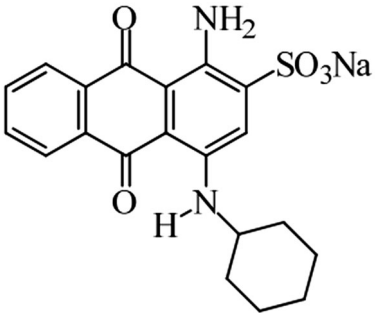

melt flow during the spinning process. The set force value was changed according to the type of formulation. It was adjusted as 5 g/min. The spinning speed was 300 m/min. No additional cooling was applied to the extrudate except for ambient conditions (at around 25 °C). The as-spun monofilaments were hot drawn with a draw ratio of 3 using heated rollers (80 °C). No heat setting was applied to the produced fiber samples. The obtained fibers had diameters of about 35 µm. For sample coding, the abbreviations PLA and OA-POSS terms are used. The sample coded as PLA/3 OA-POSS refers to the fiber sample containing 3 wt% OA-POSS.

Dyeing procedure

All dyeing processes were made according to exhaustion technique in a laboratory-type dyeing machine (Termal, Turkey) at a liquor ratio of 1:20. The general representation of dyeing procedure is shown in Fig. 3. Pristine PLA and 1 wt% OA-POSS containing fiber samples were dyed at a constant dye concentration [1% owf (on weight of fiber)] and pH (6) with varying dyeing bath temperatures (40–110 °C) and times (5–40 min). The low-melting point and the low hydrolytic stability of the PLA fiber limit the dyeing temperature and time as 110 °C and 40 min [6, 8, 9, 11]. The other parameters, OA-POSS concentration (0.5, 1 and 3 wt%) and dye concentration (0.1–5% owf) were also examined under the dyeing conditions of 100 °C and 30 min. After the dyeing process, the resulting fiber samples were rinsed with water containing nonionic surfactant at 80 °C and finally allowed to dry at room temperature.

Characterization methods

Morphology analysis

The nanomorphologies of the PLA fibers were examined using a transmission electron microscope (TEM) (Philips CM200 TEM) at an acceleration voltage of

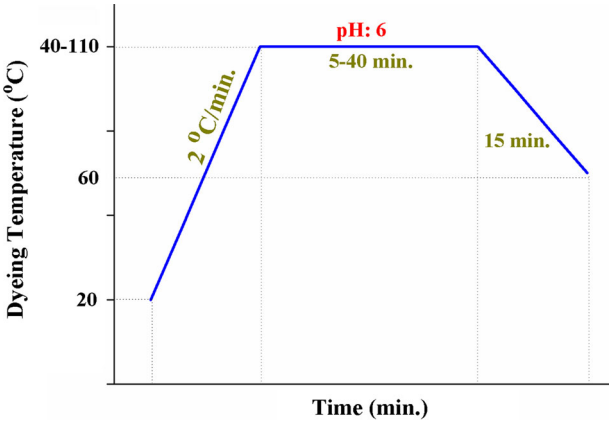

Fig. 3 The general representation of the dyeing procedure

120 kV. Ultrathin sections of 70 nm in thickness were cut with a diamond knife. All samples were trimmed parallel to the fiber forming direction. The surface morphologies of fiber samples were examined with SEM (LEO 440 computer controlled digital, 20 kV). All specimens were sputter-coated with Au/Pd before examination.

Differential scanning calorimeter

Differential scanning calorimeter analyses were used for assigning the melting point (T_m) and χ_c values of the PLA fiber samples. The percent crystallinity (χ_c) and the crystal structure are the parameters affecting the mechanical and the dyeability properties of the synthetic fibers [30, 31]. DSC analyses were performed on a Perkin Elmer Diamond under 50 ml/min nitrogen flow. Ten milligrams of samples were sealed in aluminum pans and heated from 25 to 200 °C at a heating rate of 10 °C min^{-1}. The following equation was used for the calculation of χ_c values of the PLA fiber samples.

$$\chi_c\,(\%) = \left(\Delta H_c/(1-\Phi) \times \Delta H_m^o\right) \times 100 \quad (1)$$

ΔH_c is the measured enthalpy of crystallization, ΔH_m^o is the enthalpy of 100% crystalline PLA (93 J g^{-1}) [32], Φ is the weight fraction of OA-POSS in the fiber sample.

Tensile testing

The tensile measurements of monofilaments were made using a tensile testing machine (Shimadzu AG–X) with a load cell of 10 N according the ASTM D 3822 standard. The tests were done at room temperature (about 25 °C). The sample length and the deformation rate were 20 mm and 20 mm/min, respectively. All results represent an average value of twenty tests with standard deviations. The diameters of fiber samples were measured with digital microscope (Veho VMS-004) using imaging software to calculate the stress values. The diameters of monofilaments were measured at 20 different places on the fiber sample and the average values with standard deviations are listed in Table 1.

Color measurements

The colorimetric properties of the dyeings were determined using a spectrophotometer (Minolta 3600d, Japan) coupled to a PC under D65 illuminant/10° observer with a specular component included. The fibers were measured at three locations and the results were averaged. The depth of shade was assessed in terms of the color strength (K/S) values according to the Kubelka–Munk equation:

$$K/S = (1-R)^2/2R \quad (2)$$

where K is the absorption coefficient, S is the scattering coefficient, and R is the reflectance.

Table 1 Thermal and mechanical properties of pure PLA and OA-POSS containing fibers

Sample	ϕ (μm)	T_m (°C)	ΔH_m (J/g)	χ_c (%)	σ (MPa)	ε (%)	E (GPa)
PLA	35.6 ± 1.7	166.6	40.8	43.9	259 ± 19	39 ± 15	3.2 ± 0.1
PLA/0.5 OA-POSS	36.4 ± 1.3	165.5	38.9	42.0	245 ± 17	38 ± 10	3.0 ± 0.2
PP/1 OA-POSS	37.9 ± 2.1	164.7	37.4	40.6	233 ± 15	40 ± 12	2.6 ± 0.1
PP/3 OA-POSS	36.5 ± 1.9	165.3	35.9	39.7	206 ± 21	30 ± 7	2.4 ± 0.2

ϕ fiber diameter, χ_c percent crystallinity, σ stress, ε strain, E Youngs' modulus

Wash and light fastness

The wash fastness of the fiber samples was tested using the method given in ISO 105 C06 B1S. The light fastness was made according to the ISO 105 B02 standard.

Results and discussion

Fiber morphology

The surface images of the pure and OA-POSS containing PLA fiber samples are shown in Fig. 4 at a magnification of 2000×. As seen from Fig. 4, pure PLA fiber has smooth surface structure. Tiny particles embedded into the fiber structure are seen with the addition of the OA-POSS nanoparticles. The size of these particles increases owing to the increment in the aggregation tendency of OA-POSS nanoparticles as the added amount increases. Similar agglomeration trend is observed as POSS nanoparticle concentration increases in the literature [33–37]. To observe the nanoscale dispersion of the OA-POSS nanoparticles within the PLA matrix, the TEM micrographs were analyzed (Fig. 5). OA-POSS nanoparticles are detected as dark regions owing to their high electron density [38, 39]. Although the agglomeration tendency of the OA-POSS nanoparticles increases as the concentration increases, they are dispersed at submicron size at all concentrations. It is concluded from the morphological studies that the OA-POSS is well dispersed in the PLA matrix mostly at submicron level, even some micron-sized particles existed.

DSC analysis

The DSC graphs of as-spun and drawn PLA fibers are given in Fig. 6 and the DSC data of the drawn fiber samples are listed in Table 1. As-spun PLA fibers have percent crystallinity value below 10% owing to the low fiber spinning speed (300 m/min). Similar findings are observed in the previous studies [40–42]. One melting peak is observed in all as-spun fibers. Although pure PLA fiber shows one melting peak after the hot drawing process, OA-POSS containing PLA fibers have two melting peaks owing to the formation of thinner and/or less perfect crystals.

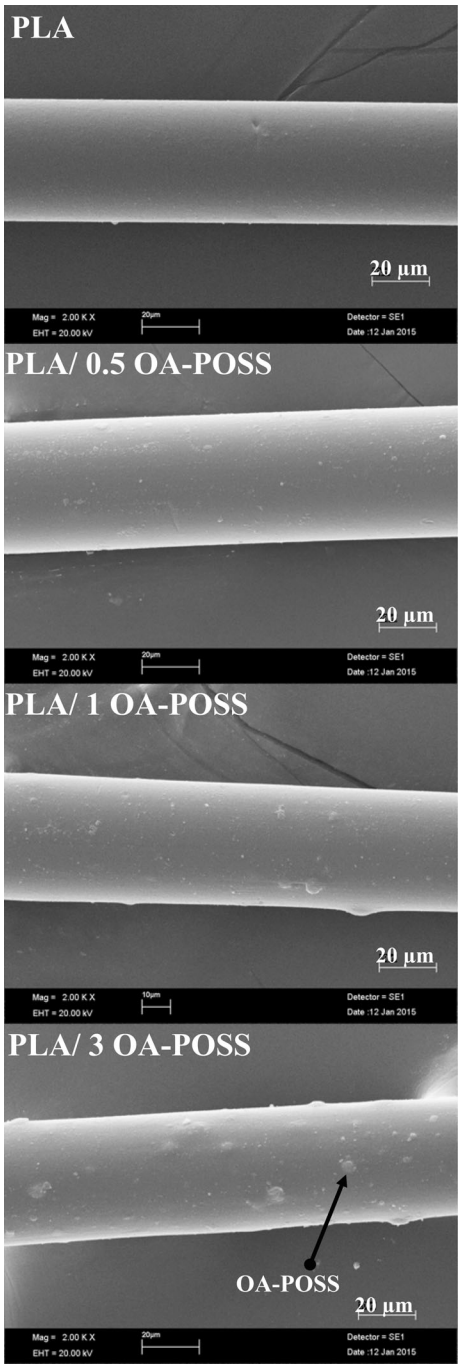

Fig. 4 The surface images of pure and OA-POSS containing PLA fiber samples at a magnification of ×2000

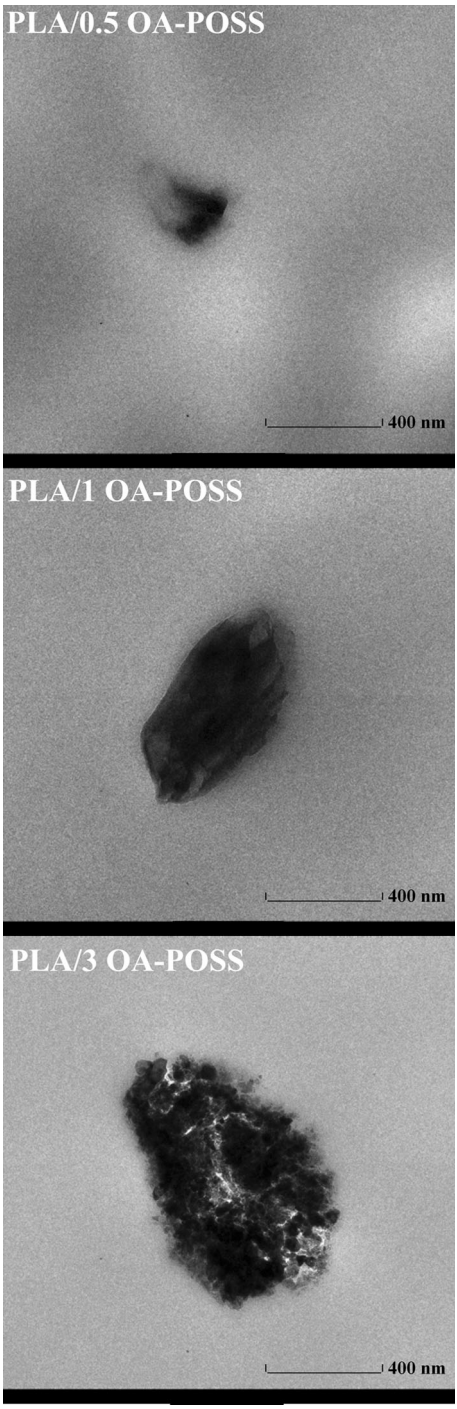

Fig. 5 TEM micrographs of modified PLA fiber samples

Similar results were observed with the addition of the *N*-phenyl aminopropyl POSS (AP-POSS) and octaaminophenyl POSS (OAP-POSS) into PLA fiber in our previous studies [16, 17]. Pristine PLA fiber has a χ_c value of 43.9%. As the added amount of the OA-POSS increases, χ_c value reduces due to the hindered formation of the ordered domains of the chains. Similar observations were found in the literature with different POSS nanoparticle matrix systems [43–46].

Tensile properties

Tensile tests were performed for investigating the effect of the OA-POSS amount on the mechanical properties of the PLA fibers. The tensile strength (σ), elongation at

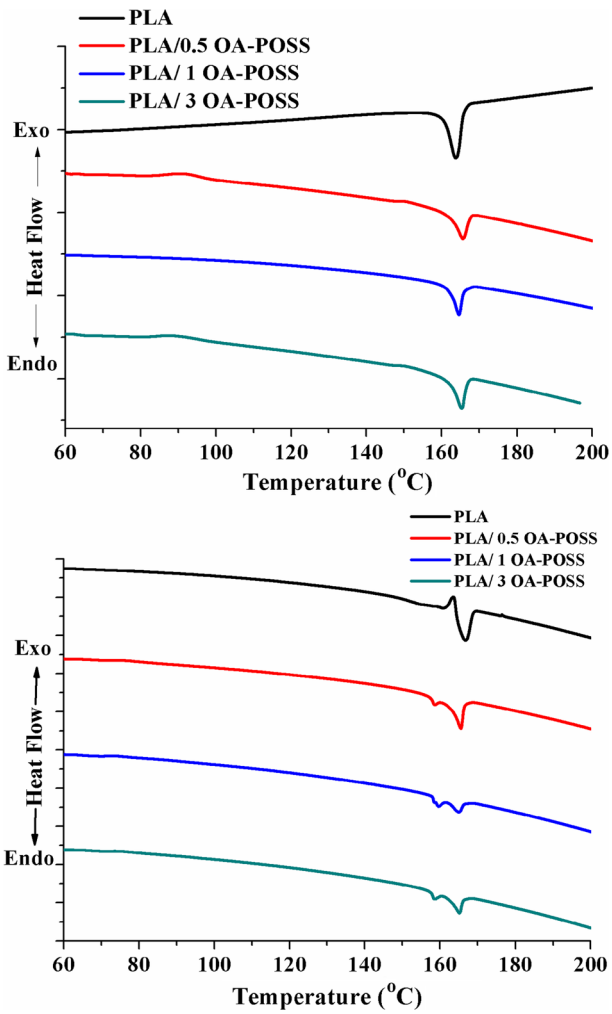

Fig. 6 DSC graphs of as-spun and drawn PLA fibers

break (ε) and Youngs' modulus (E) values of the fiber samples are given in Table 1. The σ values of the modified PLA fibers decrease at about 5.4, 10 and 20.4% with respect to pure PLA fiber with the addition of 0.5, 1 and 3 wt% OA-POSS, respectively. The E values of the modified PLA fibers reduce as the added amount of OA-POSS increases. The possible reasons for the reduction in σ and E are the formation of the weak points along the fiber axis, the reduction in χ_c and the formation of thinner and/or less perfect crystals. No significant difference is observed in the ε values of the modified PLA fiber with the addition of the OA-POSS when the standard deviations are considered.

Effect of dyeing temperature

The effect of dyeing temperature is examined using color strength (K/S) values of fiber samples. Pure and 1 wt% OA-POSS containing PLA fiber samples are dyed at different temperatures ranging from 40 to 110 °C with the increment of 10 °C for 30 min. The K/S versus temperature graphs of dyed fiber samples are shown in Fig. 7. The modified PLA fibers have higher K/S value than the pure PLA fiber at all temperatures because pure PLA fiber does not contain any dye sites to anionic dyes. The K/S value does not change when the temperature increases from 40 to 50 °C for both anionic dyes. The K/S value increases when the modified PLA fibers are dyed at 60 °C, which corresponds to the glass transition temperature of PLA, for both anionic dyes [34, 47]. The K/S value does not change when the dyeing temperature increases from 60 to 70 °C for Acid Blue 193, whereas the K/S value steadily increases as the temperature increases above 60 °C up to 100 °C for Acid Blue 62. It is thought that this trend arises from the molecular size difference between these anionic dyes. Acid Blue 193 has larger molecular size than Acid Blue 62 (Fig. 2). The larger dye molecules needs higher activation energy needed for diffusion and the larger free volume is required for dye diffusion.

Effect of dyeing time

To see the effect of dyeing time, pure and 1 wt% OA-POSS containing PLA fiber samples were dyed at 100 °C with different dyeing times of 5, 10, 20, 30 and 40 min. The K/S versus time graphs of the dyed fiber samples are shown in Fig. 8. For Acid Blue 193, K/S value increases as the dyeing time increases up to 40 min. For Acid Blue 62, K/S value increases up to 30 min. Further increment in dyeing time does not change the K/S value due to the maximum dye saturation value being reached. When the effect of dyeing time is compared according to dye type, the effect of dyeing time is more prominent with Acid Blue 193. It is thought that this observed trend arises from larger molecular size of Acid Blue 193. The time required for the diffusion of dye molecules into amorphous regions is higher for larger dye molecules.

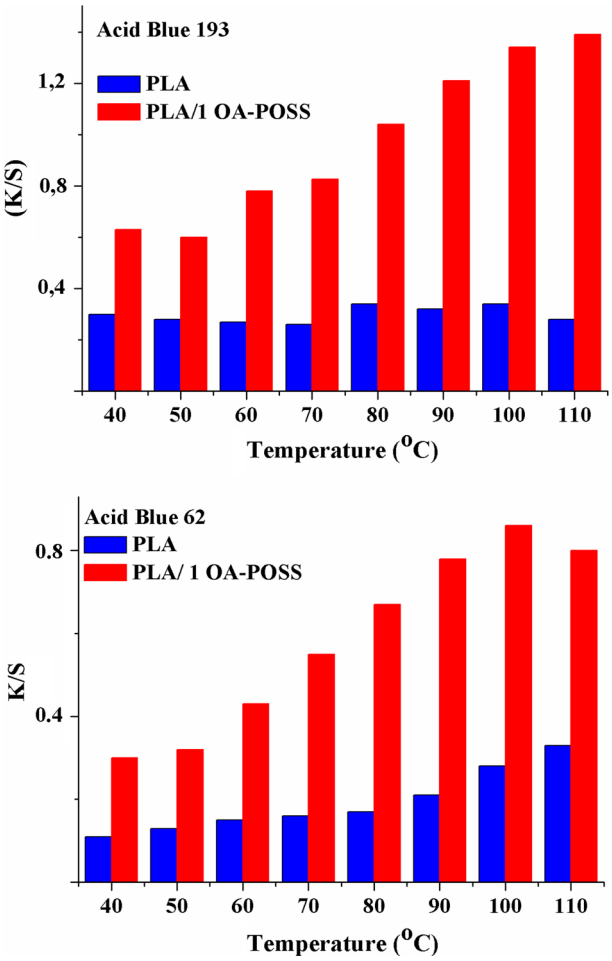

Fig. 7 *K*/*S* versus temperature graphs of dyed fiber samples

Effect of dye concentration

To see the effect of dyeing concentration, pure, 1 wt% OA-POSS containing PLA fiber samples are dyed with varying dye concentrations of 0.1, 0.5, 1, 3 and 5% owf at 100 °C for 30 min. The effect of dye concentration is examined using the *K*/*S* values of PLA fiber samples. The *K*/*S* versus dye concentration graphs of dyed fiber samples are shown in Fig. 9. Similar trend is observed with both anionic dyes. *K*/*S* value steadily increases up to 3% owf dye concentration. Negligible change is observed in *K*/*S* values of modified fibers with further increment in dye concentration. This finding implies that 3% owf dye concentration is enough for the saturation of modified PLA fibers with both anionic dyes.

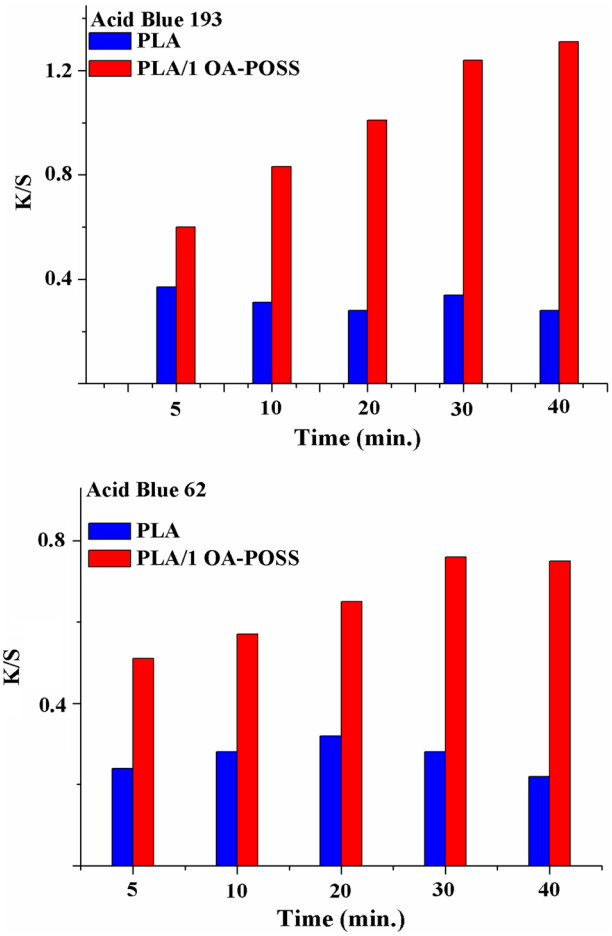

Fig. 8 *K*/*S* versus time graphs of the dyed fiber samples

Effect of POSS concentration

To examine the effect of POSS concentration (0.5, 1, 3 wt%) on the dyeability of PLA fiber, samples were dyed at 100 °C for 30 min at 3% owf dye concentration. *K*/*S* versus POSS concentration graphs of dyed fiber samples are shown in Fig. 10. The related CIELAB color coordinates (L^*, a^*, b^*, and C^*) of OA-POSS containing PLA fibers dyed are given in Table 2. The photographs of related PLA fiber samples dyed with OA-POSS are shown in Fig. 11. It is easily seen in the photographs of dyed fiber samples that pure PLA fiber has no affinity to both anionic dyes owing to the lack of dye sites for anionic dyes.

According to the dyeing results, *K*/*S* value increases and L^* value decreases as the added amount of OA-POSS nanoparticle increases. The increase in *K*/*S* values and decrease in L^* values clearly shows that the OA-POSS nanoparticle is effective for increasing the dyeability of PLA fiber with acid dyes. Acid dyes bearing one or

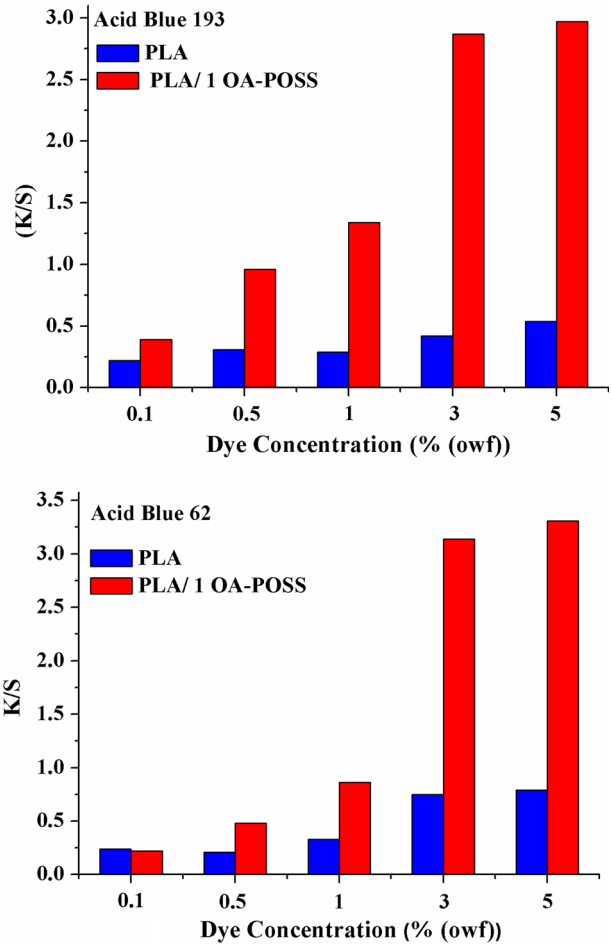

Fig. 9 *K/S* versus dye concentration graphs of dyed fiber samples

more sulphonate groups are water-soluble dyes and behave anionic character in dye bath. They migrate from aqueous dye bath and diffuse into polymer matrix. It is known that the fixation of acid dyes towards the textile fibers arises primarily from ion–ion attractions [19, 25, 48]. To favor the ion–ion interaction between acid dye and PLA fiber, the cationic group bearing POSS nanoparticle (OA-POSS) containing PLA fiber is produced. Accordingly, it is thought that the enhanced dyeability arises from the ionic interaction between the terminal ammonium groups of OA-POSS nanoparticle and the sulphonyl groups of dye molecules. The schematic representation of the proposed interaction is given in Fig. 12.

Fastness properties

The wash and light fastness of 1 wt% OA-POSS containing fibers dyed at 100 °C for 30 min with 3% owf dye concentration are shown in Table 3. The shade change

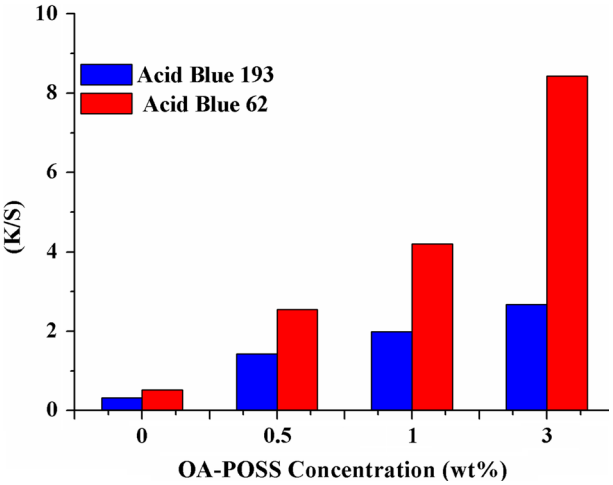

Fig. 10 *K/S* versus POSS concentration graphs of dyed fiber samples

Table 2 CIELAB color coordinates of pure and OA-POSS containing PLA fibers

Sample	*K/S*	*L**	*a**	*b**	*C*
Acid Blue 193					
PLA	0.32	80.35	−1.78	0.16	1.79
PLA/0.5 OA-POSS	1.43	56.57	−1.49	−8.53	8.66
PLA/1 OA-POSS	1.99	51.73	−0.84	−10.1	10.13
PLA/3 OA-POSS	2.62	47.14	−0.68	−10.18	10.21
Acid Blue 62					
PLA	0.52	65.65	3.11	−11.31	11.73
PLA/0.5 OA-POSS	2.55	51.2	0.31	−24.46	24.46
PLA/1 OA-POSS	4.2	45.02	2.28	−30.47	30.56
PLA/3 OA-POSS	8.43	34.94	6.15	32.73	33.3

of all PLA fibers are good (4) and fair (3) for Acid Blue 193 and Acid Blue 62, respectively. Acid Blue 62 shows lower shade change and staining on values to wool and nylon due to small molecular size. The added amount of OA-POSS does alter shade change of PLA fiber for both dyes. However, the staining on values of wool and nylon reduces as the OA-POSS concentration increases. It is thought that the reduction in staining on values arises from the high dye uptake values. The light fastness of PLA fibers does not change with the addition of OA-POSS nanoparticles regardless of their amount and remain high. The moderate or low wash fastness properties are the inherent characteristics of these dyes. In the literature, post-treatment were applied to improve the wash fastness properties [49, 50].

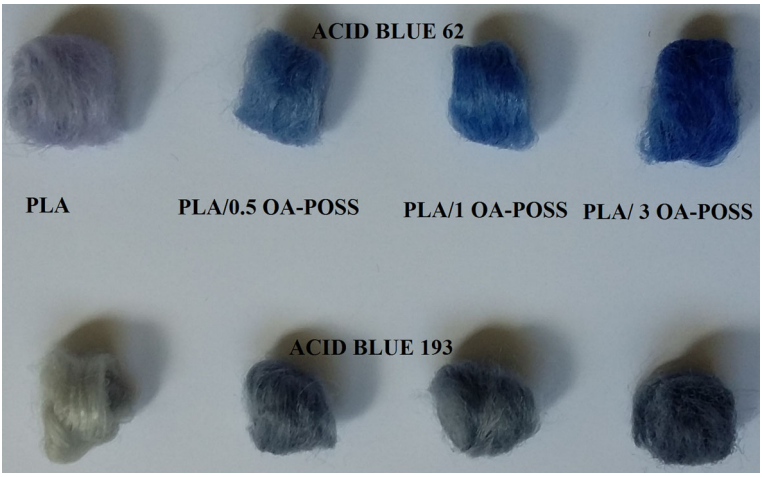

Fig. 11 The photographs of PLA fiber samples dyed with acid dyes

$$\text{Dye-SO}_3^- + {}^+{}_3\text{HN-POSS} \longrightarrow \text{Dye-SO}_3^- \cdots\cdots {}^+{}_3\text{HN-POSS}$$

Ionic attractions

Fig. 12 The schematic representation of proposed interaction between OA-POSS and acid dyes

Table 3 Wash and light fastness of pure and OA-POSS containing PLA fiber samples (dyeing conditions: pH 6, 3% owf dye concentration, 100 °C, 30 min)

Sample	Shade change	Staining on						Light fastness
		Acetate	Cotton	Nylon	PET	PAN	Wool	
Acid Blue 193								
PLA[a]	–	–	–	–	–	–	–	–
PLA/0.5 OA-POSS	4	5	5	3	4–5	5	4–5	7
PLA/1 OA-POSS	4	4–5	4–5	3	4–5	4–5	4	7
PLA/3 OA-POSS	4	4–5	4–5	2–3	4–5	4–5	4	7
Acid Blue 62								
PLA[a]	–	–	–	–	–	–	–	–
PLA/0.5 AP-POSS	3	5	5	2–3	4–5	5	3–4	7
PLA/1 AP-POSS	3	4–5	4–5	2–3	4–5	4–5	3–4	7
PLA/3 AP-POSS	3	4–5	4–5	2	4–5	4–5	3	7

[a] Pure PLA fiber did not dye with both acid dyes

Conclusion

In the current study, the dyeability of PLA fiber with anionic dyes is tried to improve with the addition of OA-POSS nanoparticles during the melt spinning. Two different anionic dyes, a disulphonated 1:2 premetallised and monosulphonated non-

metallised, are used. According to the results of morphological studies, OA-POSS is dispersed mostly at submicron level in the PLA matrix. Pure PLA fiber samples have smooth surface structure and tiny particles embedded into the fiber structure are seen with the addition of OA-POSS nanoparticles. According to the DSC results, the addition of OA-POSS promotes the formation of thinner and/or less perfect crystals after the drawing process and decreases the χ_c value as the added amount of OA-POSS increases. According to the tensile test results, both the σ and E values of OA-POSS containing PLA fibers decrease with respect to pure PLA fiber as the added amount of OA-POSS increases. It can be deduced from the dyeing results that OA-POSS is effective for increasing the dyeability of PLA fiber regardless of anionic dye type used in this study. The effectiveness of OA-POSS increases as the added amount increases. According to fastness properties, the added amount of OA-POSS does not alter the shade change and light fastness of modified PLA fiber. Whereas the staining on values of nylon and wool decrease as the OA-POSS concentration increases.

Acknowledgements This study is granted by Turkish Scientific and Technological Research Council (TUBITAK) with a Project Number of 213M268.

References

1. Perepelkin KE (2002) Polylactide fibres: fabrication, properties, use, prospects, a review. Fibre Chem 34:85–100
2. Lunt J, Bone J (2001) Properties and dyeability of fibers and fabrics produced from polylactide (PLA) polymers. AATCC Rev 1:20–23
3. Avinc O, Khoddami A (2010) Overview of poly(lactic acid)(PLA) fibre. Fibre Chem 42:68–78
4. Scheyer LE, Chiweshe A (2001) Application and performance of disperse dyes on polylactic acid (PLA) fabric. AATCC Rev 1:44–48
5. Yang Y, Huda S (2003) Comparison of disperse dye exhaustion, color yield, and colorfastness between polylactide and poly(ethylene terephthalate). J Appl Polym Sci 90:3285–3290
6. Yang Y, Huda S (2003) Dyeing conditions and their effects on mechanical properties of polylactide fabric. AATCC Rev 3:56–61
7. Choi J-H, Seo W-Y (2006) Coloration of poly(lactic acid) with disperse dyes. 1. Comparison to poly(ethylene terephthalate) of dyeability, shade and fastness. Fibers Polym 7:270–275
8. Phillips D, Suesat J, Wilding M, Farrington D, Sandukas S, Sawyer D, Bone J, Dervan S (2004) Influence of different preparation and dyeing processes on the physical strength of the Ingeo† fibre component in an Ingeo fibre/cotton blend. Part 1; scouring followed by dyeing with disperse and reactive dyes‡. Color Technol 120:35–40
9. Bilal MB, Viallier-Raynard P, Haidar B, Colombe G, Lallam A (2011) A study of the structural changes during the dyeing process of IngeoTM fibers of poly(lactic acid). Text Res J 81:838–846
10. Karst D, Nama D, Yang Y (2007) Effect of disperse dye structure on dye sorption onto PLA fiber. J Colloid Interface Sci 310:106–111
11. Karst D, Yang Y (2005) Using the solubility parameter to explain disperse dye sorption on polylactide. J Appl Polym Sci 96:416–422
12. He L, Zhang SF, Tang BT, Wang LL, Yang JZ (2007) Dyes with high affinity for polylactide. Chin Chem Lett 18:1151–1153
13. Wen H, Dai JJ (2007) Dyeing of polylactide fibers in supercritical carbon dioxide. J Appl Polym Sci 105:1903–1907
14. Burkinshaw S, Jeong D (2012) The dyeing of poly(lactic acid) fibres with disperse dyes using ultrasound: part 1–initial studies. Dyes Pigm 92:1025–1030
15. Burkinshaw S, Jeong D (2012) The dyeing of poly(lactic acid) fibres with disperse dyes using ultrasound: part 2–Fastness. Dyes Pigment 92:988–994

16. Baykuş O, Davulcu A, Dogan M (2015) Improving the dyeability of poly(lactic acid) fiber using *N*-Phenylaminopropyl POSS nanoparticle during melt spinning. Fibers Polym 16:2558–2568
17. Baykuş O, Dogan ŞD, Tayfun U, Davulcu A, Dogan M (2017) Improving the dyeability of poly(lactic acid) fiber using octa (aminophenyl) POSS nanoparticle during melt spinning. J Text Inst 108:569–578
18. Tayfun U, Dogan M (2016) Improving the dyeability of poly(lactic acid) fiber using organoclay during melt spinning. Polym Bull 73:1581–1593
19. Razafimahefa L, Chlebicki S, Vroman I, Devaux E (2008) Effect of nanoclays on the dyeability of polypropylene nanocomposite fibres. Color Technol 124:86–91
20. Razafimahefa L, Chlebicki S, Vroman I, Devaux E (2005) Effect of nanoclay on the dyeing ability of PA6 nanocomposite fibers. Dyes Pigment 66:55–60
21. Akrman J, Prikryl J (1996) Dyeing behavior of polypropylene blend fiber. I. Kinetic and thermodynamic parameters of the dyeing system. J Appl Polym Sci 62:235–245
22. Akrman J, Přikryl J (1997) Dyeing behavior of polypropylene blend fiber. II. Ionic exchange mechanism of dyeing. J Appl Polym Sci 66:543–550
23. Asiaban S, Moradian S (2012) Investigation of tensile properties and dyeing behavior of various polypropylene/polyamide 6 blends using a mixture experimental design. Dyes Pigment 92:642–653
24. Wang L-J, Hu Z-H (2009) Synthesis and application of a basic copolyamide as an acid-dyeable PTT fiber additive. Text Res J 79:1135–1141
25. Dastjerdi R, Mojtahedi M, Heidari N (2012) Developing chromic dyeable PET nanocomposites: the dye absorption and complex formation mechanisms. J Appl Polym Sci 125:3688–3694
26. Asiaban S, Moradian S (2012) Investigation of tensile properties and dyeing behavior of various polypropylene/amine modifier blends. J Appl Polym Sci 123:2162–2171
27. Fan Q, John J, Ugbolue SC, Wilson AR, Dar YS, Yang Y (2003) Nanoclay-modified polypropylene dyeable with acid and disperse dyes. AATCC Rev 3:25–28
28. Paakinaho K, Ellä V, Syrjälä S, Kellomäki M (2009) Melt spinning of poly(l/d) lactide 96/4: effects of molecular weight and melt processing on hydrolytic degradation. Polym Degrad Stab 94:438–442
29. Sirin H, Tuna B, Ozkoc G (2014) The effects of thermomechanical cycles on the properties of PLA/TPS blends. Adv Polym Technol 33
30. Yan H, Chen Y (2010) Blends of polypropylene and hyperbranched poly(phenylene sulphide) for production of dyeable PP fibres. Iran Polym J 19:791–799
31. Yu C, Zhu M, Shong X, Chen Y (2001) Study on dyeable polypropylene fiber and its properties. J Appl Polym Sci 82:3172–3176
32. Migliaresi C, Cohn D, De Lollis A, Fambri L (1991) Dynamic mechanical and calorimetric analysis of compression-molded PLLA of different molecular weights: effect of thermal treatments. J Appl Polym Sci 43:83–95
33. Butola B, Joshi M, Kumar S (2010) Hybrid organic-inorganic POSS (polyhedral oligomeric silsesquioxane)/polypropylene nanocomposite filaments. Fibers Polym 11:1137–1145
34. Sirin H, Kodal M, Ozkoc G (2016) The influence of POSS type on the properties of PLA. Polym Compos 37:1497–1506
35. Dorigato A, Pegoretti A, Migliaresi C (2009) Physical properties of polyhedral oligomeric silsesquioxanes-cycloolefin copolymer nanocomposites. J Appl Polym Sci 114:2270–2279
36. Fernandez MD, Fernandez MJ, Cobos M (2016) Effect of polyhedral oligomeric silsesquioxane (POSS) derivative on the morphology, thermal, mechanical and surface properties of poly(lactic acid)-based nanocomposites. J Mater Sci 51:3628–3642
37. Yazdaninia A, Khonakdar HA, Jafari SH, Asadi V (2016) Influence of trifluoropropyl-POSS nanoparticles on the microstructure, rheological, thermal and thermomechanical properties of PLA. RSC Adv 6:37149–37159
38. Joshi M, Butola B (2007) Isothermal crystallization of HDPE/octamethyl polyhedral oligomeric silsesquioxane nanocomposites: role of POSS as a nanofiller. J Appl Polym Sci 105:978–985
39. Yilmaz S, Kodal M, Yilmaz T, Ozkoc G (2014) Fracture toughness analysis of O-POSS/PLA composites assessed by essential work of fracture method. Compos B Eng 56:527–535
40. Gao C, Ma H, Liu X, Yu L, Chen L, Liu H, Li X, Simon GP (2013) Effects of thermal treatment on the microstructure and thermal and mechanical properties of poly(lactic acid) fibers. Polym Eng Sci 53:976–981
41. Ghosh S, Vasanthan N (2006) Structure development of poly (L-lactic acid) fibers processed at various spinning conditions. J Appl Polym Sci 101:1210–1216

42. Hossain KMZ, Parsons AJ, Rudd CD, Ahmed I, Thielemans W (2014) Mechanical, crystallisation and moisture absorption properties of melt drawn polylactic acid fibres. Eur Polym J 53:270–281
43. Baldi F, Bignotti F, Ricco L, Monticelli O, Ricco T (2006) Mechanical and structural characterization of POSS-modified polyamide 6. J Appl Polym Sci 100:3409–3414
44. Joshi M, Butola B (2004) Studies on nonisothermal crystallization of HDPE/POSS nanocomposites. Polymer 45:4953–4968
45. Sirin H, Turan D, Ozkoc G, Gurdag S (2013) POSS reinforced PET based composite fibers: "Effect of POSS type and loading level". Compos B Eng 53:395–403
46. Zeng J, Kumar S, Iyer S, Schiraldi DA, Gonzalez R (2005) Reinforcement of poly(ethylene terephthalate) fibers with polyhedral oligomeric silsesquioxanes (POSS). High Perform Polym 17:403–424
47. Kodal M, Sirin H, Ozkoc G (2014) Effects of reactive and nonreactive POSS types on the mechanical, thermal, and morphological properties of plasticized poly(lactic acid). Polym Eng Sci 54:264–275
48. Yang Y, Han S, Fan Q, Ugbolue SC (2005) Nanoclay and modified nanoclay as sorbents for anionic, cationic and nonionic dyes. Text Res J 75:622–627
49. Burkinshaw S, Son Y-A, Bide M (2001) The aftertreatment of acid dyes on nylon 6, 6 fibres: part 2. Non-metallised acid dyes. Dyes Pigments 48:209–215
50. Burkinshaw S, Son Y-A (2001) The aftertreatment of acid dyes on nylon 6, 6 fibres Part 1. 1: 2 pre-metallised acid dyes. Dyes Pigment 48:57–69